Adaptive regulation of virulence genes by microRNA-like RNAs in *Valsa mali*

Ming Xu[1] ID **, Yan Guo[1], Runze Tian[1], Chen Gao[1], Feiran Guo[1], Ralf T. Voegele[2], Jiyuan Bao[1], Chenjing Li[1], Conghui Jia[1], Hao Feng[1]** and **Lili Huang[1]** ID

[1]State Key Laboratory of Crop Stress Biology for Arid Areas and College of Plant Protection, Northwest A&F University, Yangling, Shaanxi 712100, China; [2]Department of Phytopathology, Institute of Phytomedicine, Faculty of Agricultural Sciences, University of Hohenheim, 70599 Stuttgart, Germany

Summary

• MicroRNAs play important roles in the regulation of gene expression in plants and animals. However, little information is known about the action mechanism and function of fungal microRNA-like RNAs (milRNAs).
• In this study, combining deep sequencing, molecular and histological assays, milRNAs and their targets in the phytopathogenic fungus *Valsa mali* were isolated and identified. A critical milRNA, *Vm*-milR16, was identified to adaptively regulate the expression of virulence genes.
• Fourteen isolated milRNAs showed high expression abundance. Based on the assessment of a pathogenicity function of these milRNAs, *Vm*-milR16 was found to be a critical milRNA in *V. mali* by regulating *sucrose non-fermenting 1* (*VmSNF1*), *4,5-DOPA dioxygenase extradiol* (*VmDODA*), and a *hypothetical protein* (*VmHy1*). During *V. mali* infection, *Vm*-milR16 is downregulated, while its targets are upregulated. Overexpression of *Vm*-milR16, but not mutated *Vm*-milR16, significantly reduces the expression of targets and virulence of *V. mali*. Furthermore, deletion of *VmSNF1*, *VmDODA* and *VmHy1* significantly reduce virulence of *V. mali*. All three targets seem to be essential for oxidative stress response and *VmSNF1* is required for expression of pectinase genes during *V. mali*–host interaction.
• Our results demonstrate *Vm*-milRNAs contributing to the infection of *V. mali* on apple trees by adaptively regulating virulence genes.

Introduction

RNA interference (RNAi) is a conserved mechanism to suppress gene expression by mRNA cleavage, transcriptional, or translation repression in eukaryotes (Chang *et al.*, 2012; Holoch & Moazed, 2015). There are three main kinds of conserved proteins in the RNAi pathway. Dicer or Dicer-like (DCL) proteins cleave single-stranded RNA precursors into microRNAs (miRNAs), or cleave double-stranded RNAs into small-interfering RNAs (siRNAs) (Jin & Zhu, 2010). RNA-dependent RNA polymerases (RdRPs) are involved in amplifying the silencing response (Ghildiyal & Zamore, 2009). Small RNAs (sRNAs) are then loaded into Argonaute (AGO) proteins to induce mRNA degradation, histone or DNA methylation, and translational repression by pairing of complementary sequences (Ghildiyal & Zamore, 2009; Jin & Zhu, 2010; Holoch & Moazed, 2015). RNAi was initially thought to constitute a defence mechanism against invading nucleic acids, such as transposons, transgenes, and viruses (Torres-Martínez & Ruiz-Vázquez, 2017). However, RNAi also acts as an important regulatory mechanism that affects growth, development, reproduction, and response to biotic or abiotic stresses in many eukaryotes (Ghildiyal & Zamore, 2009; Katiyar-Agarwal & Jin, 2010; Zhang *et al.*, 2011).

The phenomenon of fungal RNAi was first found in *Neurospora crassa*. Introducing fragments of *albino-1* (*al-1*), or *albino-3* (*al-3*), which are required for carotenoid biosynthesis, reduced *al-1,* or *al-3* mRNA levels and resulted in an albino phenotype (Romano & Macino, 1992). With expanding fungal genome information, RNAi pathway components were found in most fungal species (Nakayashiki *et al.*, 2006). Various work revealed that fungal RNAi plays important roles in the maintenance of genome integrity, antiviral defence and regulation of physiology, development, and virulence (Sun *et al.*, 2009; Cervantes *et al.*, 2013; Weiberg *et al.*, 2013; Raman *et al.*, 2017; Son *et al.*, 2017; Torres-Martínez & Ruiz-Vázquez, 2017; Jin *et al.*, 2019).

MicroRNAs (miRNAs) are one of the key regulators of RNAi in eukaryotes (Ghildiyal & Zamore, 2009). In 2010, miRNA-like RNAs (milRNAs), which possess the characteristics of miRNAs in plants and animals, were identified and confirmed to be generated through at least four different pathways in *N. crassa* (Lee *et al.*, 2010). In *Sclerotinia sclerotiorum*, 44 milRNA

candidates were identified and may be associated with sclerotial development (Zhou *et al.*, 2012). Twenty-seven small RNAs, which have a miRNA-like precursor structure, were identified in *Botrytis cinerea* (Weiberg *et al.*, 2013). In *Zymoseptoria tritici*, only one milRNA was identified with 85 candidate target genes involved in metabolism, cell structure, regulation of transcription, and transport (Yang, 2015). milRNAs were also identified in *Puccinia striiformis* f.sp. *tritici* (*Pst*) (Mueth *et al.*, 2015), and *Pst* milRNA1 was found to contribute to virulence by suppressing wheat pathogenesis-related 2 gene by cross-kingdom RNAi (Wang *et al.*, 2017). In addition, studies of milRNAs and their targets in *Rhizoctonia solani*, *Curvularia lunata*, and *Fusarium graminearum* suggested that milRNA may be associated with virulence and development (Chen *et al.*, 2015; Lin *et al.*, 2016; Liu *et al.*, 2016). VdmilR1, for example, can suppress target gene expression by epigenetic repression to regulate virulence of *Verticillium dahliae* (Jin *et al.*, 2019). Thus, more and more research seems to focus on the identification of milRNAs in fungi, especially in phytopathogenic fungi. However, their role in virulence and regulatory mechanisms still remains largely unknown.

The lack of suitable software to predict fungal milRNA targets and the usage of metazoan target prediction tools may hinder fungal milRNA prediction and functional exploration (Torres-Martínez & Ruiz-Vázquez, 2017). However, to thoroughly explore the biological functions of fungal milRNAs, identification of target genes is crucial. Arabidopsis sRNAs and cotton miRNAs were demonstrated to be transported into fungal cells and silence fungal target transcripts by mRNA cleavage (Zhang *et al.*, 2016; Cai *et al.*, 2018). Degradome sequencing applied in *F. graminearum* revealed that RNAi-mediated gene suppression functions at the post-transcriptional level (Son *et al.*, 2017). Therefore, mRNA cleavage mediated by endogenous milRNA may be an important pathway in fungi and targets of milRNAs may be identified based on this mechanism.

Apple Valsa canker, caused by *Valsa mali*, is one of the most severe diseases of apple trees (Wang *et al.*, 2014). The disease causes severe yield losses each year and deeply affects apple production especially in Eastern Asia (Abe *et al.*, 2007). The pathogen invades apple trees mainly through wounds or natural ostioles in the bark, and induces severe tissue maceration and necrosis (Ke *et al.*, 2013). Genome, and transcriptome sequencing, together with functional genomics revealed that many virulence factors, such as cell wall-degrading enzymes, secreted effectors, G-proteins, velvet proteins, and a PacC transcription factor are involved in virulence (Ke *et al.*, 2014; Li *et al.*, 2015; Yin *et al.*, 2015; Wu *et al.*, 2018a,b; Xu *et al.*, 2018; Zhang *et al.*, 2018). More importantly, the RNAi pathway components DCL and AGO of *V. mali* seem to be involved in stress responses and virulence (Feng *et al.*, 2017a,b), which suggests that post-transcriptional regulation may be involved in the pathogenesis of *V. mali*. In this study, deep sequencing, as well as molecular and histological assays, reveal that *V. mali* virulence is under post-transcriptional regulation mediated by *Vm*-milRNAs. Functional characterisation of *Vm*-milRNAs and corresponding targets indicates that milRNAs can adaptively regulate virulence genes to promote pathogen infection.

Materials and Methods

Strains and growth conditions

Valsa mali wild-type strain 03-8, strain Δ*VmKu80*, and *V. mali* transformants generated in this study (Table 1) are stored at the Laboratory of Integrated Management of Plant Diseases in College of Plant Protection, Northwest A&F University, China. *Valsa mali* strains were cultured on Potato Dextrose Agar (PDA) (200 g potato, 20 g dextrose, 15 g agar for 1 l) medium at 25°C in the dark. *Escherichia coli* strain DH5α used for plasmid construction was cultured on Lysogeny Broth medium at 37°C.

Sample collection and RNA extraction

In order to investigate the roles of *Vm*-milRNAs during the *V. mali*–apple bark interaction, samples of 3-d-old *V. mali* mycelium from axenic culture (MVm; *in vitro* mycelium cultured on PDA medium covered with a layer of cellophane) and material from the junction of healthy and infected apple bark tissue inoculated with *V. mali* for 3 d (IVm) were collected. Mycelial plugs (*d* = 5 mm) of *V. mali* were inoculated onto detached twigs of *Malus domestica* Borkh. cv 'Fuji' as described (Wei *et al.*, 2010). Three individual biological replicates were prepared for MVm and IVm, respectively. Total RNA were extracted with Trizol™ Reagent (Invitrogen, Carlsbad, CA, USA) following the manufacturer's instructions. RNA purity, concentration and integrity were checked. Only qualified RNA samples were used to construct cDNA libraries.

Small RNA cDNA libraries construction and high-throughput sequencing

RNA of three biological replicates of MVm, or IVm were mixed, respectively and 3 μg RNA of each sample was used for small RNA cDNA library construction. Sequencing libraries were generated using NEBNext® Multiplex Small RNA Library Prep Set for Illumina® (New England BioLabs Inc., Beverly, MA, USA) according to the manufacturer's instructions. Clustering of each index-coded sample was performed on a cBot Cluster Generation System using TruSeq SR Cluster Kit v3-cBot-HS (Illumina, San Diego, CA, USA) following the manufacturer's instructions. Libraries were sequenced on an Illumina HiSeq 2500 platform.

Identification of *Vm*-milRNAs

Raw data were processed with the Illumina pipeline filter (Solexa 0.3). Resulting data were subjected to the ACGT101-miR program (LC Sciences, Houston, TX, USA) to remove adapter dimers, junk, common RNA families, low complexity and repeats. Subsequent unique sequences with a length of 18–25 nucleotides (nt) were mapped to MIRBASE 22.0 (Kozomara & Griffiths-Jones, 2010) to identify known miRNAs and novel 3p- and 5p-derived miRNAs using BOWTIE (Langmead, 2010). The seed length was set as 16 nt and one mismatch was permitted. Unmapped sequences were blasted against the *V. mali* genome

Table 1 Wild-type and transformants of *Valsa mali* used in this study.

Strain	Description	References
WT	Wild-type strain 03-8	Yin *et al*. (2015)
Vm-milR16-OE-2	*Vm*-milR16 overexpression transformant	This study
Vm-milR16-OE-8	*Vm*-milR16 overexpression transformant	This study
Mut-R16-2	Mutated *Vm*-milR16 overexpression transformant	This study
Mut-R16-3	Mutated *Vm*-milR16 overexpression transformant	This study
EV-2	Transformant with the empty vector pDL2	This study
ΔVmKu80	VmKu80 deletion mutant	Xu *et al*. (2016)
ΔVmSNF1-3	VmSNF1 deletion mutant	This study
ΔVmSNF1-24	VmSNF1 deletion mutant	This study
EI-2	Ectopic insertion transformant of VmSNF1	This study
ΔVmDODA-8	VmDODA deletion mutant	This study
ΔVmDODA-22	VmDODA deletion mutant	This study
EI-1	Ectopic insertion transformant of VmDODA	This study
ΔVmHy1-3	VmHy1 deletion mutant	This study
ΔVmHy1-18	VmHy1 deletion mutant	This study
EI-5	Ectopic insertion transformant of VmHy1	This study
Vm-milR2, 14-OE-2	*Vm*-milR2 and *Vm*-milR14 overexpression transformant	This study
Vm-milR2, 14-OE-3	*Vm*-milR2 and *Vm*-milR14 overexpression transformant	This study
Vm-milR2, 14-OE-5	*Vm*-milR2 and *Vm*-milR14 overexpression transformant	This study
Vm-milR3, 13-OE-2	*Vm*-milR3 and *Vm*-milR13 overexpression transformant	This study
Vm-milR3, 13-OE-3	*Vm*-milR3 and *Vm*-milR13 overexpression transformant	This study
Vm-milR3, 13-OE-8	*Vm*-milR3 and *Vm*-milR13 overexpression transformant	This study
Vm-milR8, 19-OE-1	*Vm*-milR8 and *Vm*-milR19 overexpression transformant	This study
Vm-milR8, 19-OE-9	*Vm*-milR8 and *Vm*-milR19 overexpression transformant	This study
Vm-milR8, 19-OE-10	*Vm*-milR8 and *Vm*-milR19 overexpression transformant	This study
Vm-milR9, 17-OE-1	*Vm*-milR9 and *Vm*-milR17 overexpression transformant	This study
Vm-milR9, 17-OE-3	*Vm*-milR9 and *Vm*-milR17 overexpression transformant	This study
Vm-milR9, 17-OE-5	*Vm*-milR9 and *Vm*-milR17 overexpression transformant	This study
Vm-milR10, 48-OE-1	*Vm*-milR10 and *Vm*-milR48 overexpression transformant	This study
Vm-milR10, 48-OE-2	*Vm*-milR10 and *Vm*-milR48 overexpression transformant	This study
Vm-milR10, 48-OE-3	*Vm*-milR10 and *Vm*-milR48 overexpression transformant	This study

using BOWTIE (Langmead, 2010) with at most one mismatch permitted. Hairpin structure containing sequences were predicted using MFOLD (http://unafold.rna.albany.edu/?q=mfold/RNA-Folding-Form) using the parameters described (Lee *et al.*, 2010).

Only sequences which form a stem–loop structure with flanking sequences and reside in the stem regions were considered candidate milRNAs of *V. mali*.

Vm-milRNA target gene prediction, degradome sequencing and data analysis

TARGETFINDER was used to predict candidate target genes of *Vm*-milRNAs (Bo & Wang, 2005). The alignment score was set to be no more than seven. Target genes of *Vm*-milRNAs were verified by degradome sequencing. Two degradome sequencing libraries (TMVm for *V. mali in vitro* mycelium and TIVm for apple bark inoculated with *V. mali*). Total RNA (20 µg) was used to construct a degradome sequencing library following protocol of German *et al.* (2009). Poly(A)$^+$ RNA was isolated and annealed to biotinylated random primers. Streptavidin beads were used to capture biotinylated random primers labelled poly(A)$^+$ RNAs. Then, the 5′ adaptors were ligated to the poly(A)$^+$ RNAs. After reverse transcription and PCR amplification, single-end sequencing (36 bp) was performed on an Illumina HiSeq2500 at LC-BIO (Hangzhou, China). Raw reads were obtained using Illumina's PIPELINE v.1.5 software. T-plots reflecting *V. mali* transcript cleavage were analysed with CLEAVELAND3.0 (LC-BIO). Cleavage signals between 10th and 11th nucleotides (from the 5′-end of milRNA) were used to determine candidate target cleavage site of milRNA. OMICSHARE tools (http://www.omicshare.com/tools) were used for gene enrichment analyses.

Normalisation of read of *Vm*-milRNAs and their candidate target genes

The expression of *Vm*-milRNAs in MVm and IVm was normalised by transcript per million (TPM). Expression data of target genes were acquired from Ke *et al.* (2014). Reads per kilobase per million (RPKM) of candidate target genes were used for normalisation. Candidate target genes with an RPKM ratio (MVm/IVm) ≥ 2 or ≤ 0.5 were selected for co-expression analysis. Heatmaps of *Vm*-milRNAs and target genes were generated using the Heml (HEATMAP ILLUSTRATOR v.1.0; Deng *et al.*, 2014). Average linkage was used as the clustering method. Log$_2$ (TPM) values of *Vm*-milRNAs and log$_2$ (RPKM) values of target genes were used for normalisation.

Identification of virulence genes among *Vm*-milRNA target genes by PHIB-BLAST

Protein sequences of target genes of *Vm*-milRNAs were blasted to PHI-BASE 4.5 using PHIBHIB-BLAST (http://phi-blast.phi-base.org/) (Urban *et al.*, 2017). The expectation value was set as 1.0e-5. *Valsa mali* proteins which have a protein identity $\geq 30\%$ and a bit score ≥ 50 were considered candidate virulence genes.

Sequence alignment and phylogenetic analysis

Multiple sequence alignments were performed using DNAMAN software (v.7; Lynnon Corp., San Ramon, CA, USA).

Phylogenetic trees were constructed using the neighbour-joining method implemented in MEGA 7 software (Kumar *et al.*, 2016).

Relative expression of milRNAs and their corresponding target genes

Samples of *M. domestica* Borkh. cv 'Fuji' bark inoculated with *V. mali* mycelium were collected 0, 6, 12, 24, 48, 72 h post inoculation (hpi). Total RNA was extracted using the miRcute Plant miRNA Isolation Kit (Tiangen, Beijing, China) following the manufacturer's instructions. Expression of *Vm*-milRNA was detected by stem–loop qRT-PCR as described (Varkonyi-Gasic *et al.*, 2007). First-strand cDNA was synthesised by miRNA First Strand cDNA Synthesis (Stem–loop method) (Sangon Biotech, Shanghai, China) with the stem–loop RT primer, following the manufacturer's instructions. PCR detection was performed using a *Vm*-milRNA-specific forward primer and a universal reverse primer. The *V. mali* small nuclear RNA U6 was used as a control. All primers used in this study are listed in Supporting Information Table S1. For the determination of transcript levels of pri-*Vm*-milRNA, a sequence-specific primer was used for reverse transcription using the RevertAid First Strand cDNA Synthesis Kit (Thermo Scientific, Waltham, MA, USA) and following the manufacturer's instructions. Transcript levels of *V. mali* genes were analysed by qRT-PCR. First-strand cDNA was synthesised from 2 µg total RNA using the RevertAid First Strand cDNA Synthesis Kit (Thermo Scientific) and following the manufacturer's instructions. For determination of transcript levels of pri-*Vm*-milRNA and *V. mali* genes, glucose-6-phosphate dehydrogenase (*G6PDH*) of *V. mali* was used as the reference gene (Yin *et al.*, 2013). Quantitative PCR was performed using a LightCycler 96 real-time PCR machine (Roche, Basel, Switzerland) using the 2× RealStar Green Power Mixture (GenStar, Beijing, China). Relative expression of genes was calculated using the $2^{-\Delta\Delta Ct}$ method (Schmittgen & Livak, 2008).

Overexpression transformants generation of *Vm*-milRNA

For overexpression of *Vm*-milRNAs, predicted *Vm*-milRNA precursors were amplified from *V. mali* genomic DNA using Phusion High-Fidelity DNA Polymerase (New England Biolabs, Ipswich, MA, USA) and introduced into plasmid pDL2 using the ClonExpress-II One Step Cloning Kit (Vazyme Biotech, Nanjing, China). In pDL2:*Vm*-milRNA precursor constructs (Fig. S1a), milRNA precursors were expressed under the control of the *Magnaporthe grisea* ribosomal protein 27 promoter (Zhou *et al.*, 2011). Mutated *Vm*-milR16 (Mut-R16) expression constructs were generated using the Fast Site-Directed Mutagenesis Kit (Tiangen) and following the manufacturer's instructions. Constructs were verified by sequencing (Tsingke Biological Technology, Beijing, China) and transformed into *V. mali* wild-type strain 03-8 as described previously (Gao *et al.*, 2011). Transformants were screened by PCR with primer pairs outside the cloning sites of pDL2. Relative expression of *Vm*-milRNA was detected by stem–loop qRT-PCR as described above. Relative expression of *Vm*-milRNA was calculated using the $2^{-\Delta\Delta Ct}$

method (Schmittgen & Livak, 2008). A Mut-R16-specific forward primer that could discriminate exogenous Mut-R16 from endogenous *Vm*-miR16 was designed to detect the expression of Mut-R16 in Mut-R16 overexpression transformants.

Generation of target gene deletion mutants

In order to generate deletion cassettes of potential target genes and pri-*Vm*-milR16, *NEO* was amplified from plasmid pFL2 with primers *NEO*-F and *NEO*-R. *NEO* fragments were fused with specific upstream and downstream sequences of the target genes and pri-*Vm*-milR16 by double-joint PCR as described previously (Yu *et al.*, 2004). The diagram shows the strategy of gene deletion and gene deletion mutant detection used in this study (Fig. S1b). *Valsa mali* transformation was performed as described in the previous section. Gene deletion mutants were generated in strain Δ*VmKu80*, which is defective for nonhomologous end jointing (NHEJ) DNA repair. The wild-type strain 03-8 has very low gene deletion efficiency (average 1%). Δ*VmKu80* has highly enhanced target gene deletion efficiency, but no obvious differences in vegetative growth, virulence, and pycnidia formation (Xu *et al.*, 2016). For each gene or pri-*Vm*-milR16, at least two independent deletion mutants were generated and four types of PCR detections were performed to ascertain that the target gene or pri-*Vm*-milR16 was indeed replaced. A first PCR used gene or pri-*Vm*-milR16-specific primers 5F/6R to verify the deletion of the target sequence. A primer pair G852-F/G850-R designed at the inner core of *NEO* was used to verify the insertion of *NEO*. Two pairs of combined primers, gene or pri-*Vm*-milR16-specific 7F/G855-R and G856-F/gene or pri-*Vm*-milR16-specific 8R were used to ascertain the targeted homologous recombination upstream or downstream. RT-PCR was also adopted to ascertain the deletion of target genes.

Vegetative growth, stress response, virulence tests and biomass of *V. mali*

Vegetative growth of *V. mali* strains was assayed as described previously (Xu *et al.*, 2018). Briefly, mycelium plugs ($d = 5$ mm) from the edge of growing colonies were inoculated onto PDA. For oxidative stress tests, the medium was supplemented with 0.05% H_2O_2. Colony diameters were measured 2 d post cultivation (dpc). Experiments were performed three times, and each experiment included three replicates. Virulence was tested on *M. domestica* Borkh. cv 'Fuji' apple twigs and leaves by stab inoculation as described (Wei *et al.*, 2010). Lesion length or diameter was measured 4 d post inoculation (dpi). Virulence tests were repeated three times, and each experiment included at least three replicates. *Valsa mali* biomass was measured using qPCR with *V. mali*-specific *G6PDH* primers at 4 dpi. Genomic DNA was isolated using the Super Plant Genomic DNA Kit (Polysaccharides and Polyphenolics-rich) (Tiangen) from 0.4 g apple twig bark tissue including all infected tissue and additional healthy tissue following the manufacturer's instructions. Quantification of *V. mali* biomass was performed three times, and each experiment included three replicates.

Histological observation and reactive oxygen species staining

Wild-type strain and *V. mali* transformants were inoculated on *M. domestica* Borkh. cv 'Fuji' apple twigs as described above. For histological observation, infected tissue was collected at 24 hpi. Semithin sections were prepared as described previously (Ke *et al.*, 2013). Samples from the junction of infected and healthy tissue were collected and fixed in 4% glutaraldehyde in 0.1 M phosphate buffer (pH 6.8). After de-watering, samples were infiltrated with an ethanol/LR white resin mixture and pure resin (London Resin Co. Ltd, Basingstoke, UK). Semithin sections were cut from the polymerised capsules using a semithin slicer (Leica, Wetzlar, Germany) and stained with 1% (w/v) toluidine blue (Sigma, St Louis, USA). Photographs were taken using a DP72 camera (Olympus, Tokyo, Japan). Degradation area and total apple bark area were measured using IMAGEJ software (National Institutes of Health, Bethesda, MD, USA). Infection hyphae were counted and infection hyphae number per mm^2 was calculated. For reactive oxygen species (ROS) staining, apple leaves at 12 hpi were cut into pieces of 1 cm × 1 cm and immersed in 1 mg ml^{-1} 3,3 diaminobenzidine (DAB; Thermo Scientific) (pH 3.8) for 8 h under light. Samples were subsequently de-stained with ethyl alcohol : chloroform, 3 : 1 (v/v) containing 0.15% trichloroacetic acid and saturated chloral hydrate solution. Photographs were taken using a DP72 camera (Olympus). ROS accumulation was determined using IMAGEJ.

Pectinase activity tests

For each sample, 0.1 g of apple bark was collected from the junction of infected and healthy tissue at 24 hpi. Pectinase activity was tested using the pectinase activity detection kit (Solarbio, Beijing, China) following the manufacturer's instructions with a slight change: crude extracts were diluted five-fold before use. One pectinase activity unit (U g^{-1}) is defined as the 1 μmol galacturonic acid generated by breakdown of pectin per gram of sample per h under the conditions of 50°C and pH 3.5. Each pectinase assay was performed three times.

Data accessibility

Data from small RNA and degradome sequencing are available at NCBI GEO repository (GEO accession nos. GSM3757989, GSM3757990, GSM3757991 and GSM3757992).

Results

Identification and expression abundance of milRNAs in *V. mali*

In order to determine whether milRNAs are involved in the regulation of virulence in *V. mali*, two small RNA libraries were prepared from *V. mali in vitro* mycelia (MVm) and the junction of healthy and diseased apple bark inoculated with *V. mali* (IVm). Detailed information on the sequencing result is presented in Table S2. In total, 57 milRNAs were isolated from *V. mali*. In total, 56 and 15 *Vm*-milRNAs were identified in MVm and IVm, respectively (Fig. 1a; Table S3). *Vm*-milRNAs are enriched in 20, 21, and 22 nt (Fig. S2a). *Vm*-milRNAs also seem to have a strong preference for uracil in the first position of the 5′ end (Fig. S2c). Some *Vm*-milRNAs seem to share the same backbone (Table S4). Interestingly, 42 and 1 *Vm*-milRNAs are specifically expressed in MVm or IVm, respectively. There are 14 *Vm*-milRNAs expressed in both MVm and IVm (Fig. 1a; Table S3). After normalisation, we identified 14 *Vm*-milRNAs with TPM ≥ 10. *Vm*-milR15, *Vm*-milR16, *Vm*-milR22, *Vm*-milR56 and *Vm*-milR57 showed a high abundance in MVm. By contrast, *Vm*-milR1, *Vm*-milR12, *Vm*-milR19, *Vm*-milR22, *Vm*-milR56, and *Vm*-milR57 showed a high abundance in IVm (Fig. 1b; Table S3). This result might indicate that at least some *Vm*-milRNAs might be involved in the regulation of virulence.

Identification of candidate target genes related to pathogenicity of *V. mali*

Two degradome sequencing libraries (TMVm and TIVm) were constructed to identify targets of *Vm*-milRNAs. According to cleavage site characteristics of miRNAs in plants and animals, a
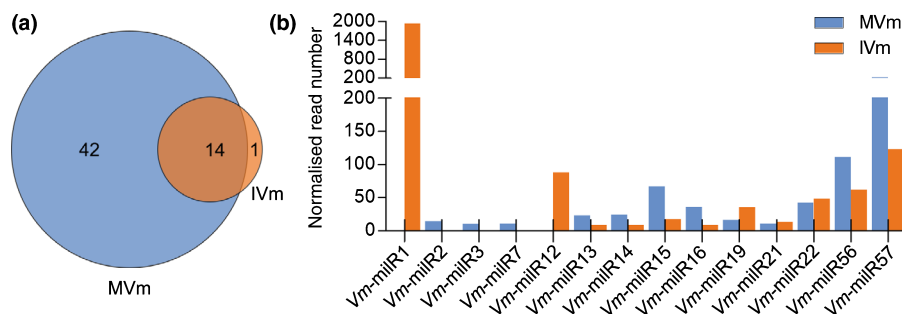
Fig. 1 *Vm*-milRNAs are differently expressed between *Valsa mali in vitro* mycelium (MVm) and apple bark infected with *V. mali* (IVm). (a) Different numbers of *Vm*-milRNAs were isolated from MVm (blue) and IVm (orange). Forty-two *Vm*-milRNAs and one *Vm*-milRNA are specifically expressed in MVm or IVm, respectively. Fourteen *Vm*-milRNAs are co-expressed in both MVm and IVm. (b) Normalised read numbers of *Vm*-milRNAs with transcript per million (TPM) ≥ 10 in either MVm (blue) or IVm (orange).

cleavage site between nucleotides 10 and 11 (from the 5′-end of milRNAs) was used to determine potential targets. In total, 356 target transcripts were detected to be potential targets of 45 *Vm*-milRNAs identified in this study (Table S5). This finding suggests that milRNA-guided mRNA cleavage might be an important way to regulate gene expression in *V. mali*. Gene ontology (GO) enrichment analysis showed that candidate target genes are enriched in cellular process, metabolic process, single-organism process, catalytic activity, binding, cell, and membrane (Figs S3, S4). *Vm*-milRNA target genes also seem to be enriched in Kyoto Encyclopedia of Genes and Genomes (KEGG) pathways for carbohydrate metabolism, translation, and transport and catabolism (Fig. S5). The expression pattern of *Vm*-milRNAs and their candidate target genes was also analysed based on the abundance of milRNAs and transcriptome information of *in vitro* mycelia and *V. mali*–apple tree interaction. Most *Vm*-milRNAs showed a negatively correlated expression with their target genes (Fig. S6).

To further determine whether milRNA target genes are involved in virulence of *V. mali*, targets were blasted to the pathogen–host interactions database (PHI-base) (Urban *et al.*, 2017). These results showed that many target genes of *Vm*-milRNAs are predicted to be virulence or lethal genes (Tables 1, S6). Thus, we speculate that *Vm*-milRNAs may affect the pathogenicity of *V. mali* by regulating the expression of virulence genes.

Vm-milRNA16 exhibits a critical role in pathogenicity

Overexpression transformants of *Vm*-milRNAs were generated to screen their function in pathogenicity. Results showed that overexpression of *Vm*-milR2, 3, 8, 9, 13, 14, 10, 16, 17, 19 and 48 could significantly reduce the virulence of *V. mali* (Fig. S7). Among these, *Vm*-milR16 overexpression transformants showed the highest decrease in virulence (Fig. S7). Additionally, pri-*Vm*-milR16 deletion mutants (Fig. S8a,b) showed normal growth *in vitro* (Fig. S8c,d), but exhibited a slight reduction in virulence (Fig. S8e,f). *Vm*-milR16 has a 64 bp putative precursor, which may form a typical hairpin structure (Fig. 2a).

Expression of three target genes could be regulated by *Vm*-milRNA16

Degradome sequencing results showed that *Vm*-milR16 is involved in the cleavage of several transcripts. Among these, VM1G_09934 was identified as a candidate virulence gene (Table 2). Two further transcripts, VM1G_10693 and VM1G_11912, seem to be upregulated during infection
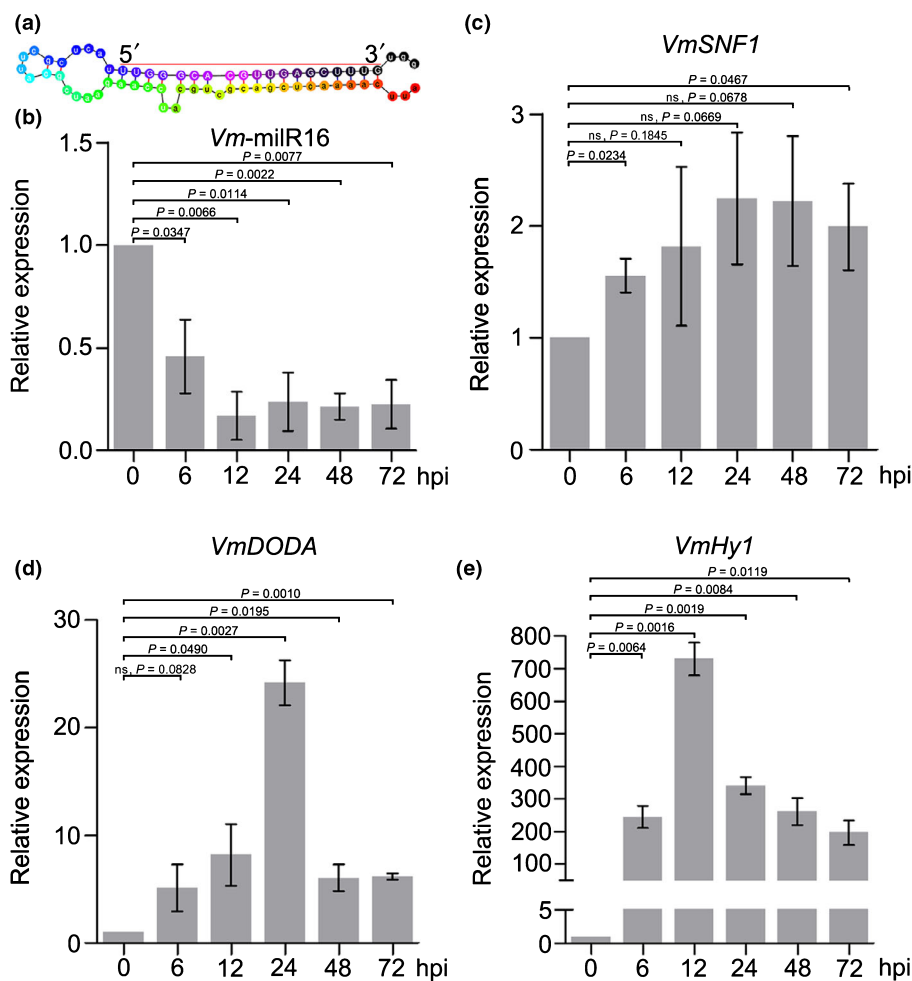
Fig. 2 Expression patterns of *Vm*-milR16 and its three target genes during *Valsa mali* infection. (a) The precursor of *Vm*-milR16 can form a hairpin structure. The red line indicates the sequence of mature *Vm*-milR16. (b) *Vm*-milR16 shows downregulation during *V. mali* infection. Relative expression levels of *Vm*-milR16 at 6, 12, 24, 48 and 72 hpi were normalised to 0 h post inoculation (hpi) (set as 1) using the $2^{-\Delta\Delta Ct}$ method. *Valsa mali* small nuclear RNA U6 (*VmU6*) was used as internal control. Data are means ±SD from three biological repeats replicates. (c–e) Relative expression of three target genes (*VmSNF1* (c), *VmDODA* (d), and *VmHy1* (e) of *Vm*-milR16 was measured with qRT-PCR. Relative expression was normalised to *VmG6PDH* and calibrated to the levels at 0 hpi (set as 1) using the $2^{-\Delta\Delta Ct}$ method. Means ± SDs were calculated from three biological replicates. Statistical analyses were performed with two-tailed *t*-test by comparing with data of 0 hpi. *P*-values are displayed on the graph. ns, no significance.

Table 2 Selection of candidate target genes identified as virulence genes of *Valsa mali* (further information can be found in Supporting Information Table S6).

milRNA	Target gene	Target gene annotation	PHI ID	Mutant description
Vm-milR6	VM1G_10013	Hypothetical protein	PHI:319	Reduced virulence
Vm-milR8	VM1G_04561	Fatty acid synthase subunit alpha	PHI:96	Loss of pathogenicity
Vm-milR9	VM1G_09360	Sphingosine-1-phosphate lyase	PHI:6886	Reduced virulence
Vm-milR9	VM1G_10041	Endothiapepsin	PHI:3973	Reduced virulence
Vm-milR10	VM1G_04374	Developmental regulator flbA	PHI:343	Loss of pathogenicity
Vm-milR13	VM1G_06797	Putative glutamate-tRNA ligase	PHI:252	Lethal
Vm-milR13	VM1G_10341	26S protease regulatory subunit 6A	PHI:1566	Lethal
Vm-milR16	VM1G_09934	Nonspecific serine/threonine protein kinase	PHI:3862	Reduced virulence
Vm-milR27	VM1G_03398	Two-component system protein A	PHI:253	Reduced virulence
Vm-milR28	VM1G_03339	Serine/threonine protein kinase nrc-2	PHI:1177	Reduced virulence
Vm-milR37	VM1G_06866	Glutathione peroxidase	PHI:5303	Reduced virulence
Vm-milR39	VM1G_10156	Hypothetical protein	PHI:429	Loss of pathogenicity
Vm-milR43	VM1G_07841	Chitin synthase regulatory factor 4	PHI:799	Reduced virulence
Vm-milR54	VM1G_00524	Transcription factor steA	PHI:268	Loss of pathogenicity
Vm-milR55	VM1G_04241	KRR1 small subunit processome component	PHI:2548	Lethal
Vm-milR57	VM1G_08759	Serine/threonine protein kinase dkf-1	PHI:680	Reduced virulence

(Fig. S6). Cleavage signals of VM1G_09934, VM1G_10693, and VM1G_11912 could be detected in *in vitro* mycelia, but no cleavage signal could be detected during *V. mali* infection (Fig. S9). Further gene annotation showed that VM1G_09934 encodes a nonspecific serine/threonine protein kinase with high similarity to *sucrose non-fermenting* 1 (*SNF1*) of *Saccharomyces cerevisiae* and several phytopathogenic fungi (Fig. S10). VM1G_09934 was accordingly termed *VmSNF1*. VM1G_10693 encodes a 4,5-DOPA dioxygenase extradiol, and was termed *VmDODA* (Fig. S11). VM1G_11912 encodes a hypothetical protein, and was termed *VmHy1*.

Relative expression was tested using stem–loop qRT-PCR and qRT-PCR in order to analyse the relationship between *Vm*-milR16 and candidate target genes. During the infection progress of *V. mali*, *Vm*-milR16 was significantly downregulated at 6, 12, 24, 48 and 72 hpi (Figs 2b, S12). Pri-*Vm*-milR16 was also significantly downregulated during *V. mali* infection (Fig. S12). All candidate target genes showed enhanced transcript levels during infection (Fig. 2c–e). Thus, the negatively correlated expression of *Vm*-milR16 and candidate target genes might indicate that *VmSNF1*, *VmDODA* and *VmHy1* could indeed be targets of *Vm*-milR16.

Vm-milRNA16 regulates target gene expression in a sequence-specific manner

To confirm the regulatory mechanism of *Vm*-milR16, mutated *Vm*-milR16 (Mut-R16) overexpression transformants were generated (Fig. 3a). Two *Vm*-milR16 overexpression transformants (OE-2 and OE-8) were confirmed to show eight-fold and six-fold enhanced transcript levels, respectively. Mut-R16 overexpression transformants did not show enhanced expression levels of *Vm*-milR16 (Fig. 3b). However, Mut-R16 was shown to be expressed in a Mut-R16 overexpression transformant (Fig. S13). Overexpression of *Vm*-milR16 resulted in a slight decrease in vegetative growth (Fig. 3c,d). Based on the lesion size and fungal biomass
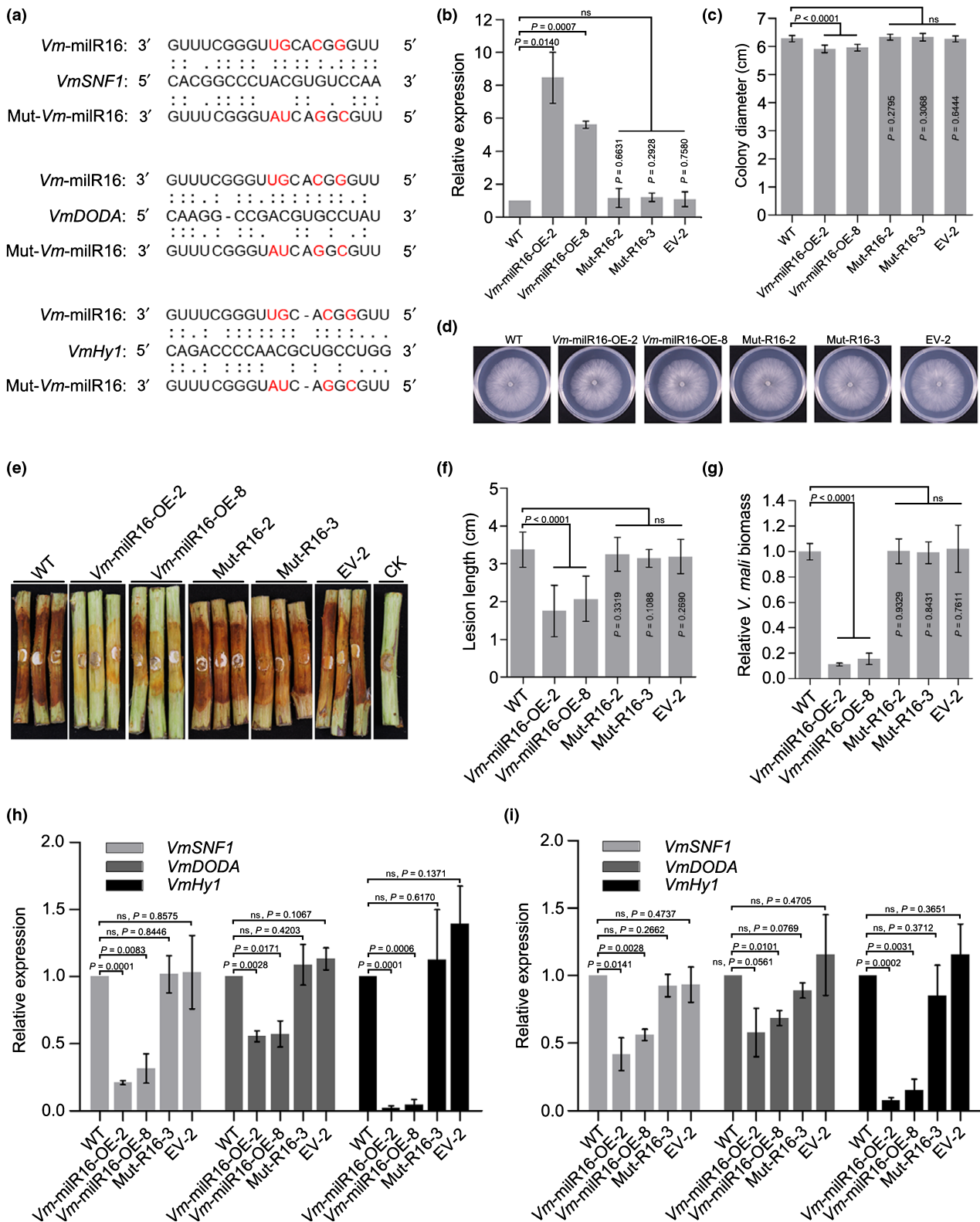
assays, overexpression of *Vm*-milR16 dramatically reduced virulence of *V. mali* (Fig. 3e–g). However, no significant change was observed when *Vm*-milR16 was mutated (Fig. 3e–g). These results confirmed our hypothesis that mature *Vm*-milR16 plays an essential role in *V. mali* virulence.

Furthermore, transcript levels of *VmSNF1*, *VmDODA* and *VmHy1* were quantified in the wild-type, *Vm*-milR16 overexpression transformants and a Mut-R16 overexpression transformant *in vitro* and during infection. Expression levels of *VmSNF1*, *VmDODA* and *VmHy1* were significantly suppressed in *Vm*-milR16 overexpression transformants, but not in the Mut-R16 overexpression transformant both *in vitro* (Fig. 3h) and *in planta* (Fig. 3i). These results suggest that *Vm*-milRNA16 regulates the expression of target genes in a sequence-specific manner.

VmSNF1, *VmDODA* and *VmHy1* are required for full virulence of *V. mali*

The reduced virulence of *Vm*-milR16 overexpression transformants and the reduced expression of target genes in *Vm*-milR16 overexpression transformants suggested that some target genes of *Vm*-milR16 may be involved in virulence of *V. mali*. Thus, *VmSNF1*, *VmDODA* and *VmHy1* deletion mutants were generated using homologous recombination (Fig. S14). At least two independent deletion mutants were obtained for each target gene. Compared with Δ*VmKu80*, all *VmSNF1*, *VmDODA* and *VmHy1* deletion mutants showed a slight reduction in vegetative growth (Fig. 4a,b). More importantly, *VmSNF1*, *VmDODA* and *VmHy1* deletion mutants showed a significant reduction in virulence (Fig. 4c–k). Moreover, the fungal biomass of *VmSNF1*, *VmDODA* and *VmHy1* deletion mutants was reduced compared with the control (Fig. 4e,h,k). These results indicated that *VmSNF1*, *VmDODA* and *VmHy1* are required for full virulence of *V. mali*.

The colonisation ability of the wild-type, *Vm*-milR16 overexpression transformants, Δ*VmKu80,* and target gene (*VmSNF1*,

(a)

Vm-milR16:   3′ GUUUCGGGUUGCACGGGUU 5′
VmSNF1:   5′ CACGGCCCUACGUGUCCAA 3′
Mut-Vm-milR16: 3′ GUUUCGGGUAUCAGGCGUU 5′

Vm-milR16:   3′ GUUUCGGGUUGCACGGGUU 5′
VmDODA: 5′ CAAGG-CCGACGUGCCUAU 3′
Mut-Vm-milR16: 3′ GUUUCGGGUAUCAGGCGUU 5′

Vm-milR16:   3′ GUUUCGGGUUGC-ACGGGUU 5′
VmHy1:   5′ CAGACCCCAACGCUGCCUGG 3′
Mut-Vm-milR16: 3′ GUUUCGGGUAUC-AGGCGUU 5′

(b) Relative expression

(c) Colony diameter (cm)

(d)

(e)

(f) Lesion length (cm)

(g) Relative V. mali biomass

(h) Relative expression

(i) Relative expression

VmDODA, and VmHy1) deletion mutants was assessed by histological observation. Wild-type and ΔVmKu80 colonised the whole cortex and caused severe tissue degradation. By contrast, only few hyphae of Vm-milR16 overexpression transformants colonised the exodermis and caused only slight tissue degradation. Meanwhile, deletion mutants of VmSNF1, VmDODA and VmHy1 also showed a reduced ability for colonisation and less tissue degradation (Fig. 5). Thus, we concluded that

Fig. 3 Overexpression of *Vm*-milR16 reduces virulence of *Valsa mali* by silencing target genes. (a) Alignment of *Vm*-milR16 and mutated *Vm*-milR16 (Mut-R16) with target genes (*VmSNF1*, *VmDODA* and *VmHy1*) at the predicted binding sites. (b) Relative expression levels of *Vm*-milR16 in the *V. mali* wild-type (WT), *Vm*-milR16 overexpression transformants (*Vm*-milR16-OE-2 and *Vm*-milR16-OE-8), Mut-R16 overexpression transformants (Mut-R16-2 and Mut-R16-3), and the empty vector transformant (EV-2). Relative expression levels of *Vm*-milR16 were normalised to *Vm*U6 and calibrated to the level of the WT (set as 1) using the $2^{-\Delta\Delta Ct}$ method. Means ± SDs were calculated from three biological replicates, each performed with three technical replicates. Error bars represent ± SDs. Colony diameter (c) and colony morphology (d) of the *V. mali* wild-type strain, *Vm*-milR16 overexpression transformants, Mut-R16 overexpression transformants, and the empty vector transformant. *Valsa mali* strains were cultured on PDA at 25°C for 2 d. Means ± SDs were calculated from nine replicates of three independent experiments. (e, f) *Vm*-milR16 overexpression transformants displayed reduced virulence compared with the wild-type and Mut-R16 overexpression transformants. Lesion lengths were measured at 4 d post inoculation (dpi). Means were calculated from three independent experiments, each containing at least three twigs. Error bars represent ± SDs. (g) *Valsa mali* biomass was measured with qPCR at 4 dpi. Relative *V. mali* biomasses were normalised to the mean of the wild-type. Means ± SDs were calculated from three biological replicates, each performed with three technical replicates. Error bars represent ± SDs. (h, i) Target genes are silenced in *Vm*-milR16 overexpression transformants, but not in a transformant carrying mutated *Vm*-milR16 *in vitro* (h) and *in planta* (24 h post inoculation, hpi) (i). Relative expression levels of *VmSNF1*, *VmDODA*, and *VmHy1* were normalised to *VmG6PDH* and calibrated to the levels of wild-type (set as 1). Means ± SD were calculated from three biological replicates, each performed with three technical replicates. Statistical analyses were performed with two-tailed *t*-test. *P*-values are displayed on the graph. ns, no significance.

downregulation of *Vm*-milR16 during *V. mali* infection results in an upregulation of virulence genes and promotes infection and colonisation.

Target genes of *Vm*-milR16 contribute to full virulence by adapting host oxidative stress responses and inducing the expression of pectinase genes

Plants can inhibit pathogen infection and colonisation by producing ROS. In this study, *Vm*-milR16 overexpression transformants and target gene (*VmSNF1*, *VmDODA* and *VmHy1*) deletion mutants showed an enhanced sensitivity to oxidative stress (Fig. 6a,b). Increased ROS accumulation was observed in apple leaves inoculated with *Vm*-milR16 overexpression transformants and target gene deletion mutants (Fig. 6c,d). This result indicated that the wild-type (and Δ*VmKu80*) can effectively scavenge ROS generated by the host. However, overexpression of *Vm*-milR16, or deletion of its target genes *VmSNF1*, *VmDODA* or *VmHy1* negatively affected the ROS scavenging ability of *V. mali*. Thus, we concluded that an enhanced expression of *VmSNF1*, *VmDODA* and *VmHy1* contributed to enhance oxidative stress responsiveness and fitness of *V. mali* during infection.

Based on the results of histological observation, the *VmSNF1* deletion mutant showed a strongly reduced ability for tissue degradation. Thus, we speculated that deletion of *VmSNF1* may affect the expression of pectinase in *V. mali*. The expression of eight pectinase genes was therefore tested in tissue inoculated with Δ*VmKu80* or a *VmSNF1* deletion mutant at 24 h. All the eight pectinase genes were significantly downregulated in the *VmSNF1* deletion mutant (Fig. 7a). Pectinase activity in apple bark tissue inoculated with Δ*VmKu80* or the *VmSNF1* deletion mutant was also measured. Similarly, pectinase activity of the *VmSNF1* deletion mutant was significantly reduced (Fig. 7b). Importantly, pectinase activity of the *Vm*-milR16 mutant was also significantly reduced compared with the wild-type (Fig. 7c). Our results indicated that *VmSNF1* participates in infection by regulating the expression of pectinase genes.

Based on the all results in this study, we postulated that many milRNAs in *V. mali* are specifically expressed or upregulated *in vitro* to suppress the expression of virulence genes. This inhibition will be relieved during pathogen–host interaction to improve

the expression of virulence genes. Therefore, we concluded that *Vm*-milRNAs adaptively regulate virulence genes in *V. mali* (Fig. 8).

Discussion

During the long arms race of plants and pathogens, plants and pathogens have evolved resistance and pathogenicity mechanism, respectively (Rodriguez-Moreno *et al.*, 2018). Plant immune responses include a series of physiological and biochemical changes, such as changes of ion fluxes, induced expression of resistance genes, bursts of ROS and production of antimicrobial compounds (Boller & He, 2009; Monaghan & Zipfel, 2012; Dangl *et al.*, 2013; Piasecka *et al.*, 2015). In parallel, plant pathogens need to be equipped with defence suppressing capabilities to reduce harm and survive during pathogen–host interactions. A large amount of research at the genome and transcriptome levels revealed the adaption of pathogenic fungi to their hosts (Dean *et al.*, 2012; van der Does & Rep, 2017). Phytopathogenic fungi have evolved an arsenal of weapons such as cell wall-degrading enzymes, toxins, and protein effectors to destroy plant tissue and interfere with host immunity (Kubicek *et al.*, 2014; Na & Gijzen, 2016; van der Does & Rep, 2017). To adapt to the host environment, phytopathogenic fungi precisely regulate gene expression at different stages to promote infection (Soyer *et al.*, 2014; van der Does & Rep, 2017).

It is generally accepted that miRNAs from plants are necessary components of plant responses to disadvantageous environmental conditions, including plant–pathogen interactions (Katiyar-Agarwal & Jin, 2010; Li *et al.*, 2017). Fungal milRNAs share common features with plant and animal miRNAs (Lee *et al.*, 2010). *Puccinia striiformis* f.sp. *tritici* for example utilises *Pst*-milRNA1 to suppress pathogenesis-related 2 gene to promote infection (Wang *et al.*, 2017). *Verticillium dahliae* milRNA1 is involved in regulating fungal virulence by transcriptional repression through enhanced histone H3K9 methylation of a gene encoding a hypothetical protein (Jin *et al.*, 2019). In this study, we show that another phytopathogenic fungus, *V. mali*, adaptively regulates its endogenous virulence genes to promote infection. Mapping the clean reads to MIRBASE 22.0, no homologous miRNAs were found. A similar result was found for *Trichoderma reesei* and
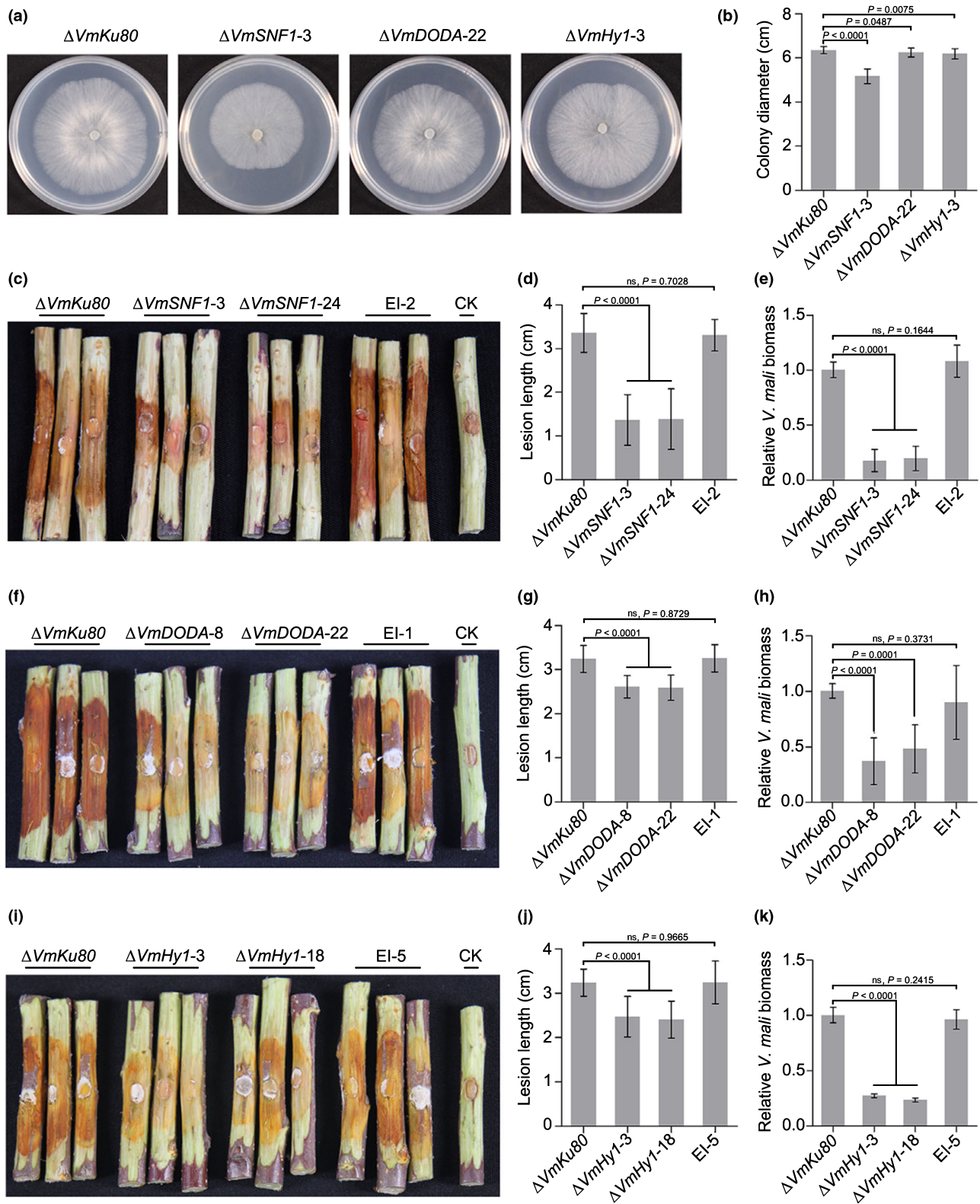
Fig. 4 Target genes of *Vm*-milR16 are required for full virulence of *Valsa mali*. Colony morphology (a) and colony diameter (b) of Δ*VmKu80* and *VmSNF1*, *VmDODA* and *VmHy1* deletion mutants. Strains were cultured on PDA at 25°C in the dark for 2 d. Means ± SDs were calculated from a total of nine replicates of three independent experiments. (c–k) *VmSNF1* (c–e), *VmDODA* (f–h) and *VmHy1* (i–k) deletion mutants exhibit reduced virulence on apple twigs as compared with strain Δ*VmKu80* and the corresponding ectopic insertion mutant. Lesion length was measured at 4 d post inoculation (dpi). In (d, g, j), means ± SDs were calculated from at least 12 replicates from three independent experiments. *Valsa mali* biomass was measured with qPCR at 4 dpi. Relative *V. mali* biomass was normalised to the mean of strain Δ*VmKu80*. In (e, h, k), means ± SDs were calculated from three biological replicates, each performed with three technical replicates. Statistical analyses were performed with two-tailed *t*-test. *P*-values are displayed on the graph. ns, no significance.
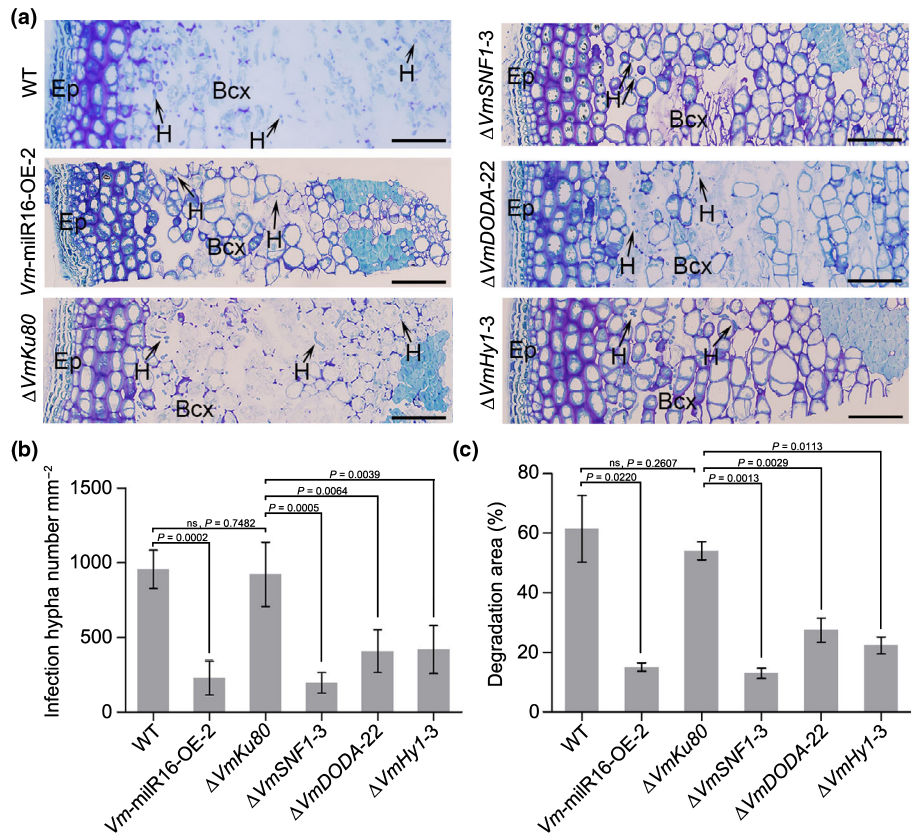
Fig. 5 *VmSNF1*, *VmDODA* and *VmHy1* are required for colonisation and tissue degradation on apple twigs in *V. mali*. (a) Representative micrographs show the colonisation and degradation of host tissue by the wild-type, *Vm*-milR16 overexpression transformant, Δ*VmKu80* and *Vm*-milR16 target gene deletion mutants on apple twigs at 24 h post inoculation (hpi). The junction of infected and healthy apple twig tissue was used for the preparation of semithin sections. Bcx, bark cortex; Ep, epidermis; H, hypha. Bars, 100 μm. Quantification of infection hyphae number (b) and percentage of degradation area (c) at 24 hpi. Means ± SDs were calculated from at least three independent replicates. Statistical analyses were performed with two-tailed *t*-test. *P*-values are displayed on the graph. ns, no significance.
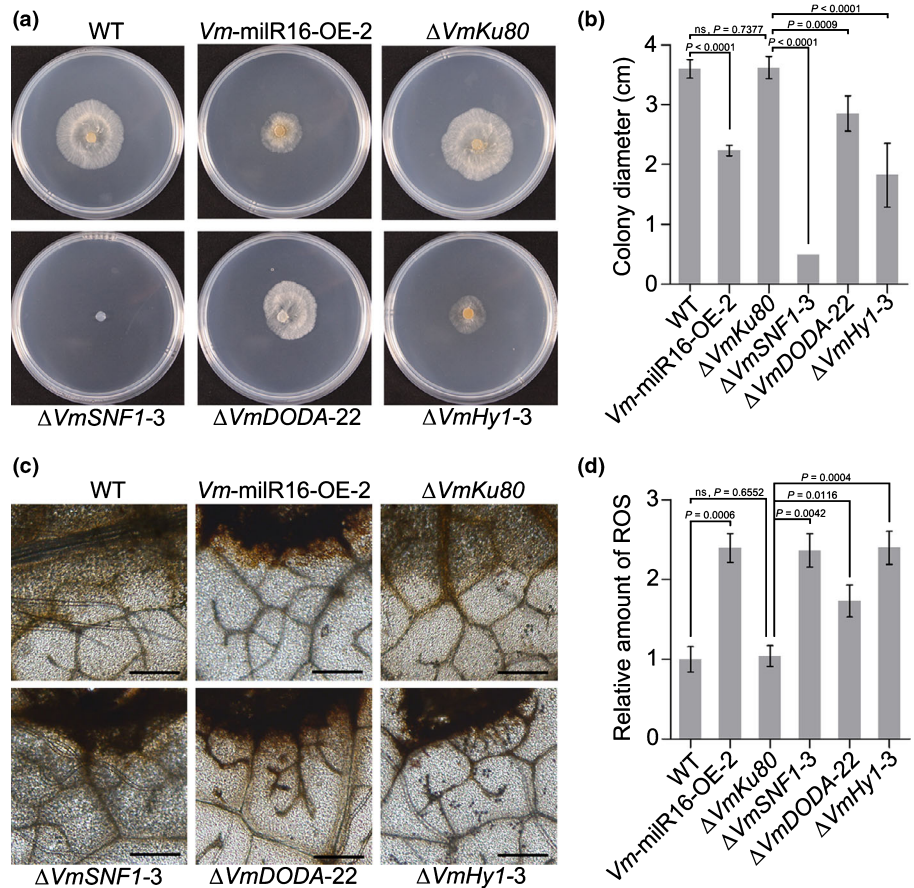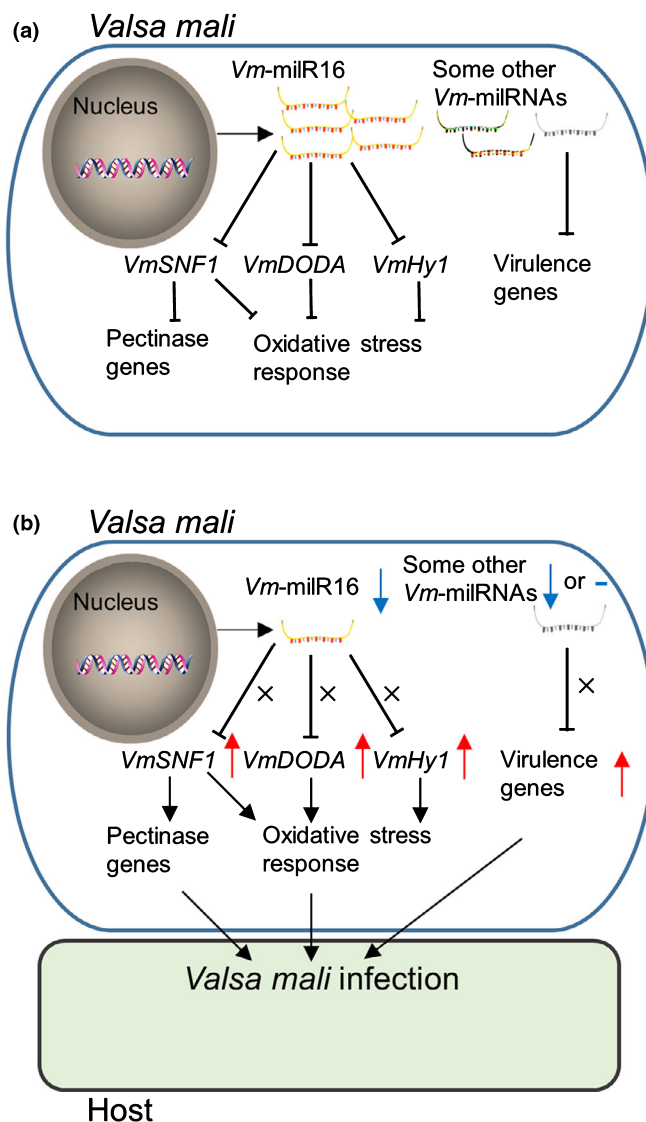
Fig. 6 *Vm*-milR16 and its target genes are involved in oxidative stress response *in vitro* and *in vivo* in *Valsa mali*. (a, b) *Vm*-milR16 overexpression transformant and *VmSNF1*, *VmDODA* and *VmHy1* deletion mutants display enhanced sensitivity to oxidative stress *in vitro*. For oxidative stress tests, mycelium plugs ($d = 5$ mm) were inoculated onto PDA supplemented with 0.05% H_2O_2 and cultured at 25°C in the dark for 2 d. Data were calculated from three biological replicates, each comprising three plates. Error bars represent ± SDs. (c, d) Apple leaves inoculated with *Vm*-milR16 overexpression transformant, Δ*VmSNF1*, Δ*VmDODA* or Δ*VmHy1* deletion mutants exhibit increased reactive oxygen species (ROS) accumulation as detected by DAB staining at 12 h post inoculation (hpi). Representative micrographs are showed. Bars, 100 μm. Quantification of ROS accumulation was performed using ImageJ. Relative ROS amounts were normalised to the mean of the wild-type. Means ± SDs were calculated from at least three biological replicates. Significance of differences was determined by two-tailed *t*-test. *P*-values are displayed on the graph. ns, no significance.
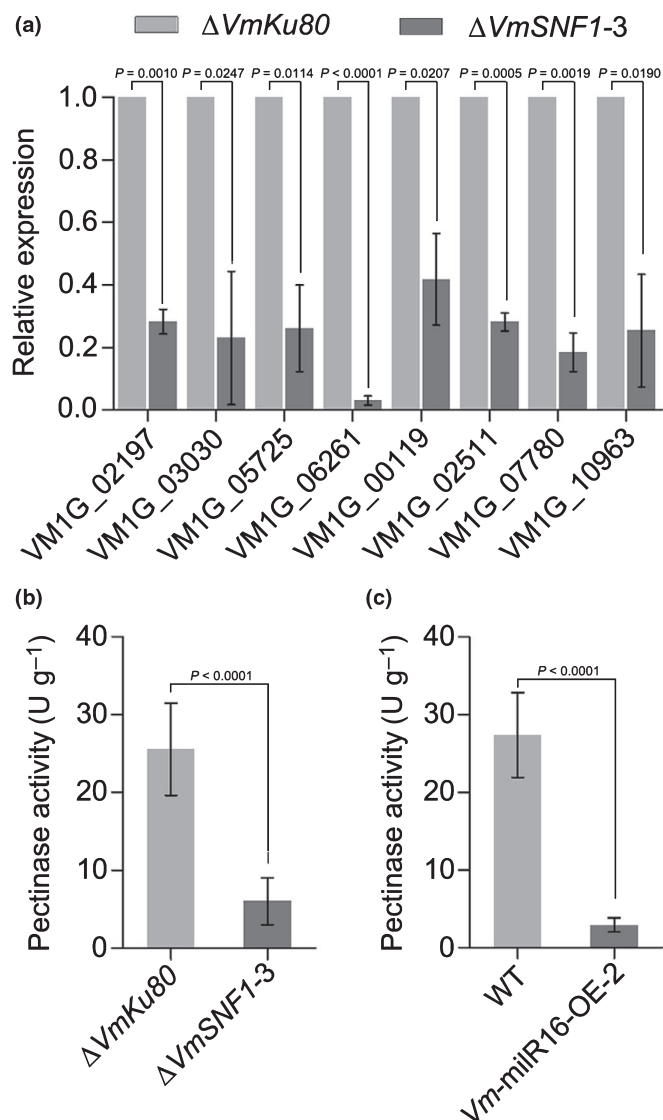
Fig. 7 *VmSNF1* is required for expression of pectinase genes during *Valsa mali* infection. (a) Transcript levels of eight pectinase genes are downregulated in a *VmSNF1* deletion mutant at 24 h post inoculation (hpi). Relative expression was normalised to *VmG6PDH* and calibrated to the levels of ΔVmKu80 (set as 1). Means ± SDs were calculated from three biological replicates, each performed with three technical replicates. Statistical significance was determined by two-tailed *t*-test. (b, c) Pectinase activity of host tissue inoculated with ΔVmKu80 or a *VmSNF1* deletion mutant tested at 24 hpi (b). Pectinase activity of host tissue inoculated with wild-type or *Vm*-milR16-OE-2 tested at 24 hpi (c). Means ± SDs were calculated from three biological replicates. Significance of differences was determined by two-tailed *t*-test. *P*-values are displayed on the graph. ns, no significance.

Fig. 8 Proposed model for the adaptive regulation of virulence genes by *Vm*-milRNAs in *Valsa mali*. *Vm*-milRNAs are involved in regulating virulence by revoking the expression of virulence genes and enhancing fitness to promote infection. (a) *In vitro*, high expression of *Vm*-milR16 and some other *Vm*-milRNAs blocks the expression of virulence genes. (b) During *V. mali* infection progress, low abundance of *Vm*-milR16 and some other *Vm*-milRNAs revokes the suppression and upregulates the virulence genes to promote the pathogen infection. Blue and red arrows represent downregulation and upregulation, respectively. The blue transverse line represents no expression.

Fusarium oxysporum (Kang *et al.*, 2013; Chen *et al.*, 2014), indicating a high degree of species specificity of fungal milRNAs.

Although many milRNAs were identified in phytopathogenic fungi (Lee *et al.*, 2010; Zhou *et al.*, 2012; Mueth *et al.*, 2015; Lin *et al.*, 2016; Zeng *et al.*, 2018), the lack of effective methods to identify target genes of milRNA has so far limited a functional exploration of milRNAs in fungi. Plants can send sRNAs into fungi and silence fungal target genes by mRNA cleavage (Zhang *et al.*, 2016; Cai *et al.*, 2018), which indicates that sRNAs-mediated mRNA cleavage exists in fungi. This mechanism can generate mRNA ends with a 5′ phosphate and these can be used for identification of milRNA target genes according to the theory of degradome sequencing (German *et al.*, 2008). Thus, degradome sequencing was also used to identify target genes of *Vm*-milRNAs. In plants and animals, the cleavage site of miRNAs is mainly located between nucleotides 10th and 11th (from 5′ to 3′ of milRNA). Based on this, the cleavage site between the 10th and 11th nucleotide was used to determine candidate target cleavage sites in this study. The generation and action mechanism of milRNAs in fungi seem to be very complex

and diverse (Lee *et al.*, 2010; Jin *et al.*, 2019). Previous studies have demonstrated that fungal transcripts are not only cleaved at the position opposite nucleotides 10 and 11 of small RNAs, but also at other positions (Zhang *et al.*, 2016; Cai *et al.*, 2018). Therefore, the targets identified in this study are only part of the real regulatory network. Targets with other cleavage sites and different mechanisms are still need to be further explored.

Vm-milR16 negatively regulates gene expression of pectinases and oxidative stress response genes by suppressing the expression of *VmSNF1*, *VmDODA*, *VmHy1 in vitro*. During infection, downregulation of *Vm*-milR16 decreases this repression, which contributes to the expression of virulence genes and enhanced fitness of *V. mali*. *VmSNF1* orthologues have been identified as essential virulence genes in phytopathogenic fungi for their function in affecting expression of cell wall-degrading enzymes (Tonukari *et al.*, 2000; Tzima *et al.*, 2011). Indeed, pectinases are also important pathogenic factors for *V. mali* (Ke *et al.*, 2013; Yin *et al.*, 2015; Wu *et al.*, 2018). *VmSNF1* deletion mutants showed greatly reduced expression levels of pectinase genes and hypersensitivity to oxidative stress. This may explain the significant reduction in virulence of *VmSNF1* deletion mutants. *VmDODA* encodes a 4,5-DOPA dioxygenase extradiol (DODA) which is a critical enzyme in betalain-related pigment biosynthesis (Girod & Zryd, 1991). Although this gene was first identified in a fungus (Hinz *et al.*, 1997), the function of *DODA* in phytopathogenic fungi remains obscure. In this study, *VmDODA* deletion mutants showed reduced virulence and an enhanced sensitivity to oxidative stress *in vitro* and *in planta*. In plants, betalains have strong ROS scavenging activity. Fungi can generate betalain-related pigments by related pathways that may be under an evolutionary convergence with plants (Polturak & Aharoni, 2018). Thus, *VmDODA* may be adaptively involved in ROS scavenging during *V. mali* infection.

In this study, we show that *V. mali* adaptively regulates virulence genes by milRNAs at the post-transcriptional level to promote infection. The results will deepen our understanding of pathogenicity mechanism of fungal pathogens, especially tree trunk disease pathogens.

Author contributions

LH, HF and MX designed the research. MX, YG, RT, CG, FG, JB, CL and CJ performed the experiments. MX, YG, RT and HF analysed the data. MX, HF, LH and RV wrote the manuscript.

ORCID

Lili Huang https://orcid.org/0000-0002-3638-9789
Ming Xu https://orcid.org/0000-0002-3415-8004

References

Abe K, Kotoda N, Kato H, Soejima J. 2007. Resistance sources to Valsa canker (*Valsa ceratosperma*) in a germplasm collection of diverse *Malus* species. *Plant Breeding* 126: 449–453.

Bo X, Wang S. 2005. TargetFinder: a software for antisense oligonucleotide target site selection based on MAST and secondary structures of target mRNA. *Bioinformatics* 21: 1401–1402.

Boller T, He SY. 2009. Innate immunity in plants: an arms race between pattern recognition receptors in plants and effectors in microbial pathogens. *Science* 324: 742–744.

Cai Q, Qiao L, Wang M, He B, Lin F, Palmquist J, Huang H, Jin H. 2018. Plants send small RNAs in extracellular vesicles to fungal pathogen to silence virulence genes. *Science* 360: 1126–1129.

Cervantes M, Vila A, Nicolás F, Moxon S, de Haro J, Dalmay T, Torres-Martínez S, Ruiz-Vázquez R. 2013. A single *argonaute* gene participates in exogenous and endogenous RNAi and controls cellular functions in the basal fungus *Mucor circinelloides*. *PLoS ONE* 8: e69283.

Chang S, Zhang Z, Liu Y. 2012. RNA interference pathways in fungi: mechanisms and functions. *Annual Review of Microbiology* 66: 305–323.

Chen R, Jiang N, Jiang Q, Sun X, Wang Y, Zhang H, Hu Z. 2014. Exploring microRNA-like small RNAs in the filamentous fungus *Fusarium oxysporum*. *PLoS ONE* 9: e104956.

Chen Y, Gao Q, Huang M, Liu Y, Liu Z, Liu X, Ma Z. 2015. Characterization of RNA silencing components in the plant pathogenic fungus *Fusarium graminearum*. *Scientific Reports* 5: 12500.

Dangl J, Horvath D, Staskawicz B. 2013. Pivoting the plant immune system from dissection to deployment. *Science* 341: 746–751.

Dean R, Van Kan J, Pretorius Z, Hammond-Kosack K, Di Pietro A, Spanu P, Dickman M, Kahmann R, Ellis J, Foster G. 2012. The Top 10 fungal pathogens in molecular plant pathology. *Molecular Plant Pathology* 13: 414–430.

Deng W, Wang Y, Liu Z, Cheng H, Xue Y. 2014. HemI: a toolkit for illustrating heatmaps. *PLoS ONE* 9: e111988.

Feng H, Xu M, Liu Y, Dong R, Gao X, Huang L. 2017a. Dicer-like genes are required for H_2O_2 and KCl stress responses, pathogenicity and small RNA generation in *Valsa mali*. *Frontiers in Microbiology* 8: 1166.

Feng H, Xu M, Liu Y, Gao X, Yin Z, Voegele R, Huang L. 2017b. The distinct roles of Argonaute protein 2 in the growth, stress responses and pathogenicity of the apple tree canker pathogen. *Forest Pathology* 47: e12354.

Gao J, Li Y, Ke X, Kang Z, Huang L. 2011. Development of genetic transformation system of *Valsa mali* of apple mediated by PEG. *Acta Microbiologica Sinica* 51: 1194–1199.

German M, Luo S, Schroth G, Meyers B, Green P. 2009. Construction of Parallel Analysis of RNA Ends (PARE) libraries for the study of cleaved miRNA targets and the RNA degradome. *Nature Protocols* 4: 356–362.

German M, Pillay M, Jeong D, Hetawal A, Luo S, Janardhanan P, Kannan V, Rymarquis L, Nobuta K, German R et al. 2008. Global identification of microRNA-target RNA pairs by parallel analysis of RNA ends. *Nature Biotechnology* 26: 941–946.

Ghildiyal M, Zamore P. 2009. Small silencing RNAs: an expanding universe. *Nature Reviews Genetics* 10: 94–108.

Girod P, Zryd J. 1991. Biogenesis of betalains: purification and partial characterization of dopa 4,5-dioxygenase from *Amanita muscaria*. *Phytochemistry* 30: 169–174.

Hinz U, Fivaz J, Girod P, Zryd J. 1997. The gene coding for the DOPA dioxygenase involved in betalain biosynthesis in *Amanita muscaria* and its regulation. *Molecular & General Genetics* 256: 1–6.

Holoch D, Moazed D. 2015. RNA-mediated epigenetic regulation of gene expression. *Nature Reviews Genetics* 16: 71–84.

Jin H, Zhu J. 2010. How many ways are there to generate small RNAs? *Molecular Cell* 38: 775–777.

Jin Y, Zhao J, Zhao P, Zhang T, Wang S, Guo H. 2019. A fungal milRNA mediates epigenetic repression of a virulence gene in *Verticillium dahliae*. *Philosophical Transactions of the Royal Society of London. Series B: Biological Sciences* 374: 20180309.

Kang K, Zhong J, Jiang L, Liu G, Gou C, Wu Q, Wang Y, Luo J, Gou D. 2013. Identification of microRNA-like RNAs in the filamentous fungus *Trichoderma reesei* by solexa sequencing. *PLoS ONE* **8**: e76288.

Katiyar-Agarwal S, Jin H. 2010. Role of small RNAs in host–microbe interactions. *Annual Review of Phytopathology* **48**: 225–246.

Ke X, Huang L, Han Q, Gao X, Kang Z. 2013. Histological and cytological investigations of the infection and colonization of apple bark by *Valsa mali* var. *mali*. *Australasian Plant Pathology* **42**: 85–93.

Ke X, Yin Z, Song N, Dai Q, Voegele R, Liu Y, Wang H, Gao X, Kang Z, Huang L. 2014. Transcriptome profiling to identify genes involved in pathogenicity of *Valsa mali* on apple tree. *Fungal Genetics and Biology* **68**: 31–38.

Kozomara A, Griffiths-Jones S. 2010. miRBase: integrating microRNA annotation and deep-sequencing data. *Nucleic Acids Research* **39**: D152–D157.

Kubicek C, Starr T, Glass N. 2014. Plant cell wall-degrading enzymes and their secretion in plant-pathogenic fungi. *Annual Review of Phytopathology* **52**: 427–451.

Kumar S, Stecher G, Tamura K. 2016. MEGA7: molecular evolutionary genetics analysis version 7.0 for bigger datasets. *Molecular Biology and Evolution* **33**: 1870–1874.

Langmead B. 2010. Aligning short sequencing reads with Bowtie. *Current Protocols in Bioinformatics* **32**: 11.7.1–11.7.14.

Lee H, Li L, Gu W, Xue Z, Crosthwaite S, Pertsemlidis A, Lewis Z, Freitag M, Selker E, Mello C et al. 2010. Diverse pathways generate microRNA-like RNAs and Dicer-independent small interfering RNAs in fungi. *Molecular Cell* **38**: 803–814.

Li S, Castillo-González C, Yu B, Zhang X. 2017. The functions of plant small RNAs in development and in stress responses. *The Plant Journal* **90**: 654–670.

Li Z, Yin Z, Fan Y, Xu M, Kang Z, Huang L. 2015. Candidate effector proteins of the necrotrophic apple canker pathogen *Valsa mali* can suppress BAX-induced PCD. *Frontiers in Plant Science* **6**: 579.

Lin R, He L, He J, Qin P, Wang Y, Deng Q, Yang X, Li S, Wang S, Wang W et al. 2016. Comprehensive analysis of microRNA-Seq and target mRNAs of rice sheath blight pathogen provides new insights into pathogenic regulatory mechanisms. *DNA Research* **23**: 415–425.

Liu T, Hu J, Zuo Y, Jin Y, Hou J. 2016. Identification of microRNA-like RNAs from *Curvularia lunata* associated with maize leaf spot by bioinformation analysis and deep sequencing. *Molecular Genetics and Genomics* **291**: 587–596.

Monaghan J, Zipfel C. 2012. Plant pattern recognition receptor complexes at the plasma membrane. *Current Opinion in Plant Biology* **15**: 349–357.

Mueth N, Ramachandran S, Hulbert S. 2015. Small RNAs from the wheat stripe rust fungus (*Puccinia striiformis* f. sp. *tritici*). *BMC Genomics* **16**: 718.

Na R, Gijzen M. 2016. Escaping host immunity: new tricks for plant pathogens. *PLoS Pathogens* **12**: e1005631.

Nakayashiki H, Kadotani N, Mayama S. 2006. Evolution and diversification of RNA silencing proteins in fungi. *Journal of Molecular Evolution* **63**: 127–135.

Piasecka A, Jedrzejczak-Rey N, Bednarek P. 2015. Secondary metabolites in plant innate immunity: conserved function of divergent chemicals. *New Phytologist* **206**: 948–964.

Polturak G, Aharoni A. 2018. "La Vie En Rose": Biosynthesis, sources, and applications of betalain pigments. *Molecular Plant* **11**: 7–22.

Raman V, Simon S, Demirci F, Nakano M, Meyers B, Donofrio N. 2017. Small RNA functions are required for growth and development of *Magnaporthe oryzae*. *Molecular Plant–Microbe Interactions* **30**: 517–530.

Rodriguez-Moreno L, Ebert M, Bolton M, Thomma B. 2018. Tools of the crook-infection strategies of fungal plant pathogens. *The Plant Journal* **93**: 664–674.

Romano N, Macino G. 1992. Quelling: transient inactivation of gene expression in *Neurospora crassa* by transformation with homologous sequences. *Molecular Microbiology* **6**: 3343–3353.

Schmittgen T, Livak K. 2008. Analyzing real-time PCR data by the comparative CT method. *Nature Protocols* **3**: 1101–1108.

Son H, Park A, Lim J, Shin C, Lee Y. 2017. Genome-wide exonic small interference RNA-mediated gene silencing regulates sexual reproduction in the homothallic fungus *Fusarium graminearum*. *PLoS Genetics* **13**: e1006595.

Soyer J, El Ghalid M, Glaser N, Ollivier B, Linglin J, Grandaubert J, Balesdent M, Connolly L, Freitag M, Rouxel T et al. 2014. Epigenetic control of effector gene expression in the plant pathogenic fungus *Leptosphaeria maculans*. *PLoS Genetics* **10**: e1004227.

Sun Q, Choi G, Nuss D. 2009. A single Argonaute gene is required for induction of RNA silencing antiviral defense and promotes viral RNA recombination. *Proceedings of the National Academy of Sciences, USA* **106**: 17927–17932.

Tonukari N, Scott-Craig J, Walton J. 2000. The *Cochliobolus carbonum* SNF1 gene is required for cell wall-degrading enzyme expression and virulence on maize. *Plant Cell* **12**: 237–248.

Torres-Martínez S, Ruiz-Vázquez R. 2017. The RNAi universe in fungi: a varied landscape of small RNAs and biological functions. *Annual Review of Microbiology* **71**: 371–391.

Tzima A, Paplomatas E, Rauyaree P, Ospina-Giraldo M, Kang S. 2011. *VdSNF1*, the sucrose nonfermenting protein kinase gene of *Verticillium dahliae*, is required for virulence and expression of genes involved in cell-wall degradation. *Molecular Plant–Microbe Interactions* **24**: 129–142.

Urban M, Cuzick A, Rutherford K, Irvine A, Pedro H, Pant R, Sadanadan V, Khamari L, Billal S, Mohanty S et al. 2017. PHI-base: a new interface and further additions for the multi-species pathogen–host interactions database. *Nucleic Acids Research* **45**: D604–D610.

van der Does H, Rep M. 2017. Adaptation to the host environment by plant-pathogenic fungi. *Annual Review of Phytopathology* **55**: 427–450.

Varkonyi-Gasic E, Wu R, Wood M, Walton E, Hellens R. 2007. Protocol: a highly sensitive RT-PCR method for detection and quantification of microRNAs. *Plant Methods* **3**: 12.

Wang B, Sun Y, Song N, Zhao M, Liu R, Feng H, Wang X, Kang Z. 2017. *Puccinia striiformis* f. sp. *tritici* microRNA-like RNA 1 (*Pst*-milR1), an important pathogenicity factor of *Pst*, impairs wheat resistance to *Pst* by suppressing the wheat pathogenesis-related 2 gene. *New Phytologist* **215**: 338–350.

Wang X, Zang R, Yin Z, Kang Z, Huang L. 2014. Delimiting cryptic pathogen species causing apple Valsa canker with multilocus data. *Ecology and Evolution* **4**: 1369–1380.

Wei J, Huang L, Gao Z, Ke X, Kang Z. 2010. Laboratory evaluation methods of apple Valsa canker disease caused by *Valsa ceratosperma* sensu Kobayashi. *Acta Phytopathologica Sinica* **40**: 14–20.

Weiberg A, Wang M, Lin F, Zhao H, Zhang Z, Kaloshian I, Huang H, Jin H. 2013. Fungal small RNAs suppress plant immunity by hijacking host RNA interference pathways. *Science* **342**: 118–123.

Wu Y, Xu L, Yin Z, Dai Q, Gao X, Feng H, Voegele R, Huang L. 2018a. Two members of the velvet family, *VmVeA* and *VmVelB*, affect conidiation, virulence and pectinase expression in *Valsa mali*. *Molecular Plant Pathology* **19**: 1639–1651.

Wu Y, Yin Z, Xu L, Feng H, Huang L. 2018b. *Vm*PacC is required for acidification and virulence in *Valsa mali*. *Frontiers in Microbiology* **9**: 1981.

Xu M, Gao X, Chen J, Yin Z, Feng H, Huang L. 2018. The feruloyl esterase genes are required for full pathogenicity of the apple tree canker pathogen *Valsa mali*. *Molecular Plant Pathology* **19**: 1353–1363.

Xu M, Yin Z, Gao M, Lu W, Gao X, Huang L. 2016. Construction of enhanced gene deletion frequency recipient strain Δ*VmKu80* in *Valsa mali*. *Acta Agriculturae Boreali-occidentalis Sinica* **25**: 298–305.

Yang F. 2015. Genome-wide analysis of small RNAs in the wheat pathogenic fungus *Zymoseptoria tritici*. *Fungal Biology* **119**: 631–640.

Yin Z, Ke X, Huang D, Gao X, Voegele R, Kang Z, Huang L. 2013. Validation of reference genes for gene expression analysis in *Valsa mali* var. *mali* using real-time quantitative PCR. *World Journal of Microbiology and Biotechnology* **29**: 1563–1571.

Yin Z, Liu H, Li Z, Ke X, Dou D, Gao X, Song N, Dai Q, Wu Y, Xu J et al. 2015. Genome sequence of Valsa canker pathogens uncovers a potential adaptation of colonization of woody bark. *New Phytologist* **208**: 1202–1216.

Yu J, Hamari Z, Han K, Seo J, Reyes-Domínguez Y, Scazzocchio C. 2004. Double-joint PCR: a PCR-based molecular tool for gene manipulations in filamentous fungi. *Fungal Genetics and Biology* **41**: 973–981.

Zeng W, Wang J, Wang Y, Lin J, Fu Y, Xie J, Jiang D, Chen T, Liu H, Cheng J. 2018. Dicer-like proteins regulate sexual development via the biogenesis of perithecium-specific microRNAs in a plant pathogenic fungus *Fusarium graminearum*. *Frontiers in Microbiology* **9**: 818.

Zhang M, Feng H, Zhao Y, Song L, Gao C, Xu X, Huang L. 2018. *Valsa mali* pathogenic effector *Vm*PxE1 contributes to full virulence and interacts with the host peroxidase *Md*APX1 as a potential target. *Frontiers in Microbiology* 9: 821.

Zhang T, Zhao Y, Zhao J, Wang S, Jin Y, Chen Z, Fang Y, Hua C, Ding S, Guo H. 2016. Cotton plants export microRNAs to inhibit virulence gene expression in a fungal pathogen. *Nature Plants* 2: 16153.

Zhang X, Zhao H, Gao S, Wang W, Katiyar-Agarwal S, Huang H, Raikhel N, Jin H. 2011. Arabidopsis Agonaute 2 regulates innate immunity via miRNA393*-mediated silencing of a Golgi-localized SNARE gene, *MEMB12*. *Molecular Cell* 42: 356–366.

Zhou J, Fu Y, Xie J, Li B, Jiang D, Li G, Cheng J. 2012. Identification of microRNA-like RNAs in a plant pathogenic fungus *Sclerotinia sclerotiorum* by high-throughput sequencing. *Molecular Genetics and Genomics* 287: 275–282.

Zhou X, Li G, Xu J. 2011. Efficient approaches for generating GFP fusion and epitope-tagging constructs in filamentous fungi. In: Xu JR, Bluhm B, eds. *Fungal genomics. Methods in molecular biology (methods and protocols)*. Totowa, NJ, USA: Humana Press, 199–212.

Supporting Information

Additional Supporting Information may be found online in the Supporting Information section at the end of the article.

Fig. S1 Schematic diagram for the generation of *Vm*-milRNA overexpression constructs and gene deletions.

Fig. S2 Sequence characteristics of *Vm*-milRNAs.

Fig. S3 GO enrichment of candidate *Vm*-milRNA target genes.

Fig. S4 Bubble diagram of GO enriched terms in biological process, molecular function, and cellular component.

Fig. S5 KEGG pathway enrichment and enriched bubble diagram of top 25 KEGG pathway of candidate *Vm*-milRNA target genes.

Fig. S6 Correlated expression pattern analysis of *Vm*-milRNAs and candidate target genes in *in vitro* mycelium (MVm) and apple bark inoculated with *V. mali* (IVm).

Fig. S7 *Vm*-milR16 plays a critical role in pathogenicity of *V. mali* on *M. domestica* Borkh. cv 'Fuji'.

Fig. S8 Deletion of pri-*Vm*-milR16 enhances virulence of *V. mali*.

Fig. S9 Three target genes of *Vm*-milR16 were identified by degradome sequencing.

Fig. S10 Multiple sequence alignment and phylogenetic analysis of *VmSNF1* (*Valsa mali* KUI74329.1).

Fig. S11 Multiple sequence alignment and phylogenetic analysis of *VmDODA* (*Valsa mali* KUI63952.1).

Fig. S12 *Vm*-milR16 and pri-*Vm*-milR16 are downregulated during *V. mali* infection.

Fig. S13 Mutated *Vm*-milR16 (Mut-R16) can be detected in the overexpression transformant (Mut-R16-3), but not in the wild-type (WT), the *Vm*-milR16 overexpression transformant (*Vm*-milR16-OE-2), or the empty vector transformant (EV-2).

Fig. S14 Detection of target gene deletion mutants by four PCR and RT-PCR reactions.

Table S1 Primers used in this study.

Table S2 Results of small RNAs sequencing of *in vitro* mycelium (MVm) and apple bark inoculated with *V. mali* (IVm).

Table S3 *Vm*-milRNAs identified in this study and their expression levels.

Table S4 Cluster index of pre-miRNAs.

Table S5 Target genes of *Vm*-milRNAs identified by degradome sequencing and analysis.

Table S6 Candidate virulence genes identified from *Vm*-milRNA target genes.

Please note: Wiley-Blackwell are not responsible for the content or functionality of any supporting information supplied by the authors. Any queries (other than missing material) should be directed to the *New Phytologist* Central Office.